Cancer/Radiothérapie 24 (2020) 128–134

Disponible en ligne sur
ScienceDirect
www.sciencedirect.com

Elsevier Masson France
EM|consulte
www.em-consulte.com

Original article

Monte Carlo dose calculations of shielding disks with different material combinations in intraoperative electron radiation therapy (IOERT)

Calculs de dose de Monte-Carlo des disques de blindage avec différentes combinaisons de matériaux en radiothérapie électronique peropératoire

H. Alhamada[a,b,*], S. Simon[a,b], C. Philippson[b], C. Vandekerkhove[b], Y. Jourani[b], N. Pauly[a,b], D. Van Gestel[b], N. Reynaert[b]

[a] *Nuclear Metrology, école polytechnique, université Libre de Bruxelles, Bruxelles, Belgium*
[b] *Radiothérapy Department, institut Jules-Bordet, Bruxelles, Belgium*

ARTICLE INFO

Article history:
Received 10 September 2019
Received in revised form 10 February 2020
Accepted 12 February 2020

Keywords:
Monte Carlo (MC)
Intraoperative electron radiation therapy (IORT)

ABSTRACT

Purpose. – Shielding disks play an important role in intraoperative electron radiation therapy, and different designs are currently used in clinical practice. This paper investigates the dosimetric impact of the shielding disk used during intraoperative electron radiation therapy (IOERT).
Materials and Methods. – This paper focuses on the study of four shielding disks types that have been used in our clinic: Aluminum (Al)/Lead (Pb), PMMA/Copper(Cu)/PMMA, Aluminum (Al)/Copper (Cu) and Aluminum (Al)/Steel with their specific thicknesses. The theoretical study was conducted with the EGSnrc Monte Carlo (MC) code. On the other hand, the measurements were carried out with gafchromic films for the four shielding disks for the same setup inside the water phantom. Finally, a comparison of the simulated and measured PDD curves was performed for the four material combinations.
Results. – MC simulation and gafchromic measurements illustrated that dose values under the four shielding disks types were close to 0, whereas the backscattering enhancement of the disks were 103% with Al/Pb shielding disk, 102% with Al/Steel shielding disk, 102% with Al/Cu shielding disk, 95% with PMMA/Cu/PMMA shielding disk. The PDDs values of the gafchromic films in front of the disks were: 107%, 105%, 104%, and 94% for the Al/Pb, Al/Steel, Al/Cu, and PMMA/Cu/PMMA disks respectively.
Conclusions. – The dose values above and under the shielding disks were acceptable for the four studied shielding types. Demonstrated it is possible to use any of them clinically, while the best shielding disk was the Al/Pb since it has minimum thickness and a small backscatter enhancement.

Mots clés :
Monte-Carlo
Radiothérapie peropératoire par électrons

RÉSUMÉ

Objectif de l'étude. – Les disques de protection jouent un rôle important dans la radiothérapie peropératoire. Différents modèles de ces disques sont actuellement utilisés en clinique. Cet article étudie l'impact dosimétrique du disque de blindage utilisé lors de la radiothérapie électronique peropératoire.
Matériels et méthodes. – Quatre types de disques de blindage utilisés dans notre clinique ont été étudiés : aluminium (Al)/plomb (Pb), PMMA/cuivre (Cu)/PMMA, Al/Cu et Al/acier avec leurs épaisseurs spécifiques. L'étude théorique a été réalisée avec le code EGSnrc Monte-Carlo. Les mesures ont été effectuées avec des films gafchromiques pour les quatre disques de blindage, cela pour une même configuration à l'intérieur du fantôme d'eau. Enfin, une comparaison des courbes PDD simulées et mesurées a été effectuée pour les quatre combinaisons de matériaux.

* Corresponding author at: Nuclear Metrology, école polytechnique, université Libre de Bruxelles, Bruxelles, Belgium.
E-mail address: husein.alhamada@ulb.ac.be (H. Alhamada).

https://doi.org/10.1016/j.canrad.2020.02.006
1278-3218/

Résultats. – La simulation Monte-Carlo et les mesures par film gafchromiques ont montré que les valeurs de dose sous les quatre types de disques de blindage étaient proches de 0, alors que la rétrodiffusion des disques était de 103 % en utilisant le disque de blindage Al/Pb, de 102 % en utilisant le disque de blindage Al/acier, de 102 % en utilisant le disque de blindage Al/Cu et de 95 % en utilisant le disque de blindage PMMA/Cu/PMMA. Les valeurs de PDD des films gafchromiques situés devant les disques étaient de 107 %, 105 %, 104 % et 94 % et respectivement pour les disques Al/Pb, Al/acier, Al/Cu et PMMA/Cu/PMMA.
Conclusions. – Les valeurs de dose au-dessus et sous les disques de protection étaient acceptables pour les quatre types de protection étudiés. Cela démontre qu'il est possible d'utiliser n'importe lequel d'entre eux pour la routine clinique. Le meilleur choix de blindage est cependant l'alliage Al/Pb, car il possède une épaisseur minimale et une faible amélioration de la rétrodiffusion.

1. Introduction

Intraoperative radiation therapy (IOERT) is a radiotherapy technique performed inside the operation room during surgery. Its goal is to deliver a high dose (10–20 Gy) directly to the tumor bed or to the residual tumor in a single session [1].

IOERT technique has many advantages:

- direct visual control of the treated volume;
- possibility of keeping healthy tissues away from high dose areas [2];
- short treatment time, and;
- delivery of a high dose to the tumor bed, where microscopic cancer infiltration may be present after tumor removal, in order to decrease the local tumor recurrence risk [3].

Breast cancer treated with an IOERT boost dose or with a full dose, therefore replacing external radiotherapy, is currently reported to be the main IOERT procedure [4,5]. Unfortunately, treatment planning based on the real patient anatomy during the surgery is still an issue and the treatment parameters (applicator size and type, beam energy, bolus thickness, monitor units) have to be determined and computed inside the operating room. During the IOERT of the breast, insertion of a shielding disk between the residual breast and the pectoral fascia protects the organs underneath like the ribs, lung and heart [6,7]. The shielding disk is usually composed of 2 layers: the second layer is made of a high-Z material (steel, copper, lead) that stops the electron beam whereas the main function of the first layer, made of a low-Z material (PMMA, aluminum), is to absorb most of the backscattered radiation produced by the second layer [8]. The choice of the optimal shielding disk is a compromise between clinical practice, requiring a thin disk, and dose conformity. Therefore, a standard is not defined, and a high number of different shielding disks are used in clinical practice, mostly based on personal preference.

Neto et al. used two layers shielding disk (Al/Pb) with electron beam energy 12 MeV [9]. Russo et al. confirmed that (3 mm Al/2 mm Pb) is optimal for the NOVAC7 IOERT machine, which its maximum energy is 10 MeV [10]. According to Pentiricci et al. study PTFE & Stainless-Steel disk provides better attenuation characteristics compared to the PMMA ones [11]. Hanna et al. tried a three layers shielding disk (3 mm Silicon/3 mm Al/3 mm Pb) to minimize the backscatter to target volume [12]. Severgnini et al used a 7 mm PMMA/3 mm Cu disk for the 12 MeV electron beam energy of the Mobetron 1000 [6]. Alhamada et al used (4 mm Al/3 mm Pb) as a shielding disk with 12 MeV and they developed a new technique to avoid misalignments between the applicator and the shielding disk [13].

The main aim of this work is to study the dosimetric impact of different shielding disk types with IOERT and to verify the suitability of these shielding disks for clinical usage based on MC simulation and gafchromic film measurements.

2. Material and methods

2.1. Linear Accelerator

The mobile accelerator Mobetron 1000 (IntraOp Medical Inc., Sunnyvale, CA) is designed to be used in unshielded operation rooms. It may be moved in or out, from side to side in the horizontal plane (±5 cm) and moved up and down in the vertical plane. It may be tilted in the radial plane and rotated in the transverse plane. All movements are motorized and controlled by a wired hand pendant. The nominal source surface distance (SSD) is 50 cm and the gantry rotation axis height is approximately 99 cm above the floor [14,15]. Four nominal electron beam energies are available (4, 6, 9 and 12 MeV). Opposite to the accelerator and tracking the beam direction, a beam stopper decreases the stray radiation underneath the operating theater to an acceptable level.

The design of the Mobetron 1000 allows for safe usage with 12 MeV electron energy beams in an unshielded operation room up to a 250 Gy weekly workload [16,17].

The accelerator comes with 45 cylindrical Al/steel applicators, with 3 to 10 cm diameters in 0.5 cm steps. The exit angle is flat (0°) or beveled (15° or 30°). This gives the opportunity to choose the most adequate applicator according to the treated area size and location [18,19].

2.2. MC Simulation settings

The accelerator head was modeled using the EGSnrc/BEAMnrc simulation package and the dose distribution in the water phantom was calculated with the DOSXYZnrc code [20–23]. This study was performed for our most clinically used flat applicator (5.5 cm diameter) and for the maximum energy available (12 MeV). Fig. 1 shows the modeled components of the Mobetron 1000.

For all simulations, the water phantom was a ($10\,cm \times 10\,cm \times 10\,cm$) cube size of H2O521ICRU material with 1 mm voxel size. Transport and particles production threshold energy for electrons (ECUT, AE) were set to 521 KeV and for photons (PCUT, AP) set to 10 KeV. ECUT and AE include the rest mass of the electron. The source 9 of DOSXYZnrc was used to calculate the deposited dose of the particles (photon, electron or positron) in water phantom to minimize calculation time and to avoid using a big phase-space file. Statistical uncertainty was less than 1% for 100 million initial particles inside the field. The calculation time took roughly 10 hours per simulation by using a dedicated Cluster (2.9 GHz/64 cores/128 Gb RAM). For all the simulations, PRESTA-II was used as an Electron-step algorithm

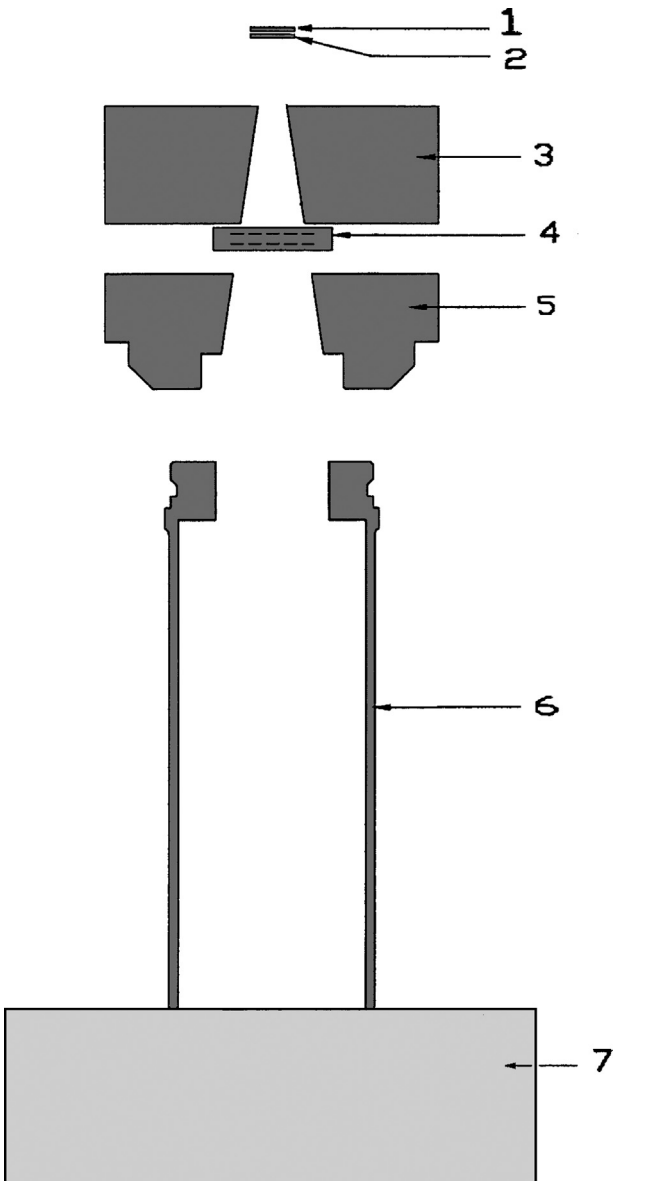

Fig. 1. Schematic overview of the Mobetron 1000 geometry as modeled with BEAMnrc (1: electron source, 2: scattering foil, 3: first collimator, 4: ion monitor chamber, 5: second collimator, 6: applicator, 7: water phantom).

The PRESTAII algorithm takes into account lateral and longitudinal correlations in a condensed history step [24].

2.3. MC Model Tuning

PDD measurements during the commissioning were mainly performed with the flat ionization chamber (Roos chamber, PTW, Freiburg, Germany). The ionometric data were corrected for relative water to air stopping-power ratios variation with energy and for ion recombination. The PDDs were also compared with curves obtained from other detectors such as the Diamond detector (PTW, Freiburg, Germany), Diode-E detector (PTW, Freiburg, Germany) and a 0.125 cm^3 thimble ionization chamber (Semiflex chamber, PTW, Freiburg, Germany). Dose profiles were performed with the Diode-E detector. All measurements were performed with the applicator in contact with the water surface (no air gap). Due to the absence of any crosshair in the field, the positioning of the detector exactly at the center is not straightforward. The center of the field is determined by performing in-plane and cross-plane dose profile measurements at the nominal D_{max}.

The MC model tuning process is the main time-consuming process in the simulation of the linear accelerator head. It includes the matching of the MC simulation results with standard measurements by finding the correct properties of the initial electron beam. The properties of the initial electron beam are the energy spectrum and the spot size of the source. Iterative changing of mean energy and full width at half maximum (FWHM) of the Gaussian source profile is the common method for the tuning process of conventional accelerators [25,26]. This method is not so effective in our study since there is no bending magnet in the Mobetron 1000 accelerator head and, consequently, the resulting spectrum always contains low energy components. MC model tuning was done according to Iaccarino approach [27]. The tuning approach was done by calculating PDDs with mono-energetic electrons in the range from 1 MeV up to 13 MeV with a step of 0.5 MeV. The weight factor was calculated by equation 1 for each mono-energy value. The optimization continues until optimal weight values W_j that provide the minimum of the objective value. The energy spectrum is determined by the mono energy weights in the spectrum.

The objective value=

$$\sum_i \| \sum_j D_j^c \left(Z_j\right) * W_j - d^m \left(Z_i\right) \|^2 \quad (1)$$

$(Z_i)\, D_j^c$ is the MC calculated PDD for mono energy (j), $d^m\,(Z_i)$ is the measured PDD and $W_j\ (\geq 0)$ is the weight of energy (j) in the spectrum to obtain the minimum difference between MC and measured values.

2.4. Shielding disk simulations

No standard design is provided for shielding disks. Some disks are provided by the manufacturers while others are developed by the users to better fit their specific needs. The summary of the shield designs, based on collected data from different international centers, is shown in Table 1.

Four types of shielding disks of 7 cm diameter have been simulated in our institution: 4 mm Al/4 mm Steel, 4 mm Al/3 mm Pb, 6 mm PMMA/3 mm Cu/1 mm PMMA and 6 mm Al/3 mm Cu. In the MC simulations, all the shielding disks were positioned in a water phantom at 36 mm depth (90% isodose line of the 12 MeV beam) and aligned perpendicularly with the beam axis. MC simulations had the same setup as the gafchromic film measurements as illustrated in Fig. 2.

2.5. Gafchromic film measurements

The EBT3 films (Ashland Inc. Covington, KY USA) have been chosen for our study because of their high spatial resolution, their small influence of the depth on the calibration curves, their weak dependence on beam energy and their small sensitivity to daylight. EBT gafchromic films could be used for an absolute dose determination when they are positioned parallel to the electron beam [28–30]. EBT3 film measurements have been used to validate the MC simulations. The determination of the calibration curve is the first step to use the gafchromic films for measurements. Seven strips of films were irradiated with doses ranging from 0 to 25 Gy. Twenty-four hours were allowed to elapse prior to scanning to allow stabilization of the development process. The films were positioned in the same orientation and in the central area of the scanner where the response is more uniform [31,32]. They were scanned using a flatbed scanner EPSON 750XL, in transparency mode. The calibration curve was established with the FilmQAPro software. For the PDD measurements, four gafchromic film pieces with dimensions of (10×3.6) cm were placed in a vertical plane in a water phantom.

Table 1
Specifications of shielding disks used in some international centers.

Materials: Thickness [mm]	Diameters [cm]	Maximum Backscatter	Maximum Transmission	Reference
PMMA: 7/Cu: 3 /PMMA: 2	6, 7, 8, 9, 10	9 MeV: < 1% 12 MeV: < 1%	9 MeV: < 1% 12 MeV: < 1%	[36]
Lucite 10	3–10 in 0.5 increments	NR*	12 MeV: ~15% of D90	[39]
Al: 6/Cu: 3	7, 8 used most frequently	12 MeV: < 10%	6 MeV: ~0.5% 9 MeV: ~1% 12 MeV: < 15%	[39]
Al: 3/Pb: 3	4–8	NR*	12 MeV: < 5%	[39]
Al: 4/Pb: 4	7	12 MeV: ~10%	12 MeV: ~6% of D90	[39]
Al: 6/Cu: 3	NR	9 MeV: 6% 12 MeV: 6%	9 MeV: 1.2% 12 MeV: 2%	[8]
Al: 4/Pb: 4	4, 5, 6, 7, 8, 9	NR*	NR*	[40]
Al: 5/Pb: 4	4, 5, 6, 7, 8, 10	NR*	NR*	[41]

NR*: not reported.

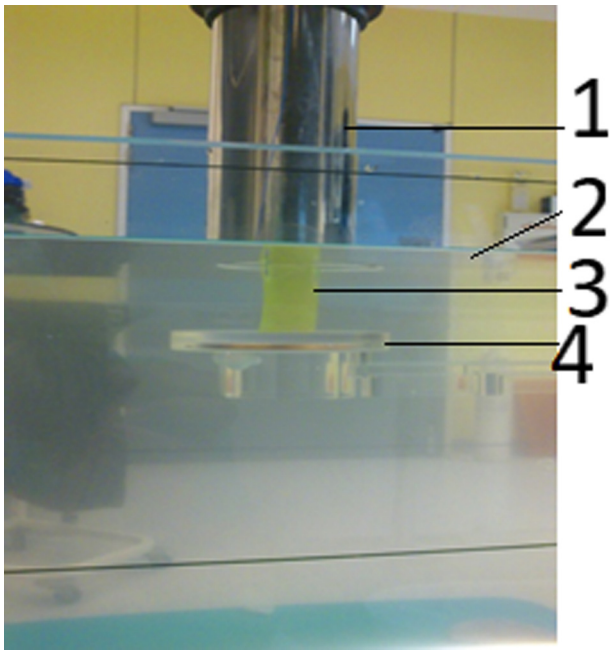

Fig. 2. Setup of gafchromic film measurement: 1: the applicator, 2: water phantom, 3: the gafchromic film stands vertically between the applicator and shielding disk, 4; the 6 mm PMMA/3 mm Cu/1 mm PMMA shielding disk.

One piece was used for each disk at the same set-up, they were stuck perpendicularly between the shielding disk and the 5.5 cm applicator tip which was in contact with the water surface as illustrated in Fig. 2. One film, used for the tuning process, (10 cm × 8 cm) was irradiated with the same set-up of Fig. 2 but without any disk. Other strips of films were attached horizontally under the shielding disks to measure the dose beneath the shielding. They were exposed to a 12 MeV beam. All the gafchromic films were analyzed with the red channel using the same protocol that was used for the calibration curve.

With a tuned MC model of the 12 MeV beam, we were able to assess the dosimetric impact of the shielding disks. The PDDs, with shielding disks, are presented in Fig. 6. The MC results were normalized to the maximum dose of MC modelling without the shielding disk and the results of gafchromic films were normalized to the maximum dose of the film without the shielding disk. The gafchromic films, placed beneath the shielding disks, show that there is no radiation under the disk.

3. Results

3.1. Measurements and tuning process

In Fig. 3, a comparison is provided between PDDs obtained with gafchromic film and various detectors. Except for the Diode-E, which gives a slight shift towards bigger depths of PDD, all PDD measurements are matched for the different detectors.

The spectrum of electrons corresponding to our 12 MeV measurements has a mean energy of 12.43 MeV with a FWHM of 0.2 cm for the Gaussian source in the MC model. The value of the root mean square deviation (RMSD) is about 2.2% between PDD of MC simulation and PDD of measurements. The statistical uncertainties of MC simulation of the PDD as illustrated in Fig. 4 are 2% at 1 mm depth, 0.2% at D_{max} and 2.8% at 75 mm depth. The uncertainties of the MC simulation of the dose profile at D_{max} (=27 mm for 12 MeV) varied from 0.3% inside the applicator up to 2% outside the field. The spectrum of the initial electron source before hitting any part of MC model is illustrated in Fig. 5.

3.2. Shield disk simulations and gafchromic film measurements

Fig. 6 illustrates the PDDs of gafchromic films in the actual treatment set-up for the four shielding disk types. The measurements of gafchromic films stop at 36 mm depth due to the presence of the shielding disk. The PDDs of gafchromic films at the borders of the shielding disks are 107%, 105% and 105% for the Al/Pb, Al/Steel and Al/Cu disks respectively, and 94% for the PMMA/Cu/PMMA shielding disk. MC PDDs show that all the simulated shielding types, if they are positioned at the 90% isodose depth, had the required thickness to minimize the dose percentage of the primary radiation down to less than 2%. Furthermore, most of the backscattering radiation from high-Z material is absorbed by the upper layer. PDDs of the MC at the surface entrance disks are 103%, 102% and 102% for the Al/Pb, Al/Steel and Al/Cu disks respectively, and 95% for the PMMA/Cu/PMMA shielding disk. All simulations of the shielding disk types have statistical uncertainty inside the field of less than 1%.

As illustrated in Fig. 6, PDDs after all studied shielding disks are almost 0.

4. Discussion

IOERT dosimetry is considered as a challenge, due to the 10–20 Gy delivered to the target area in a single session including the difficulty of pretreatment planning. For tuning an MC model, many approaches can be considered, such as direct measurement by inserting a film close to the initial electrons source, then the energy spectrum is obtained by a deconvolution algorithm, but this

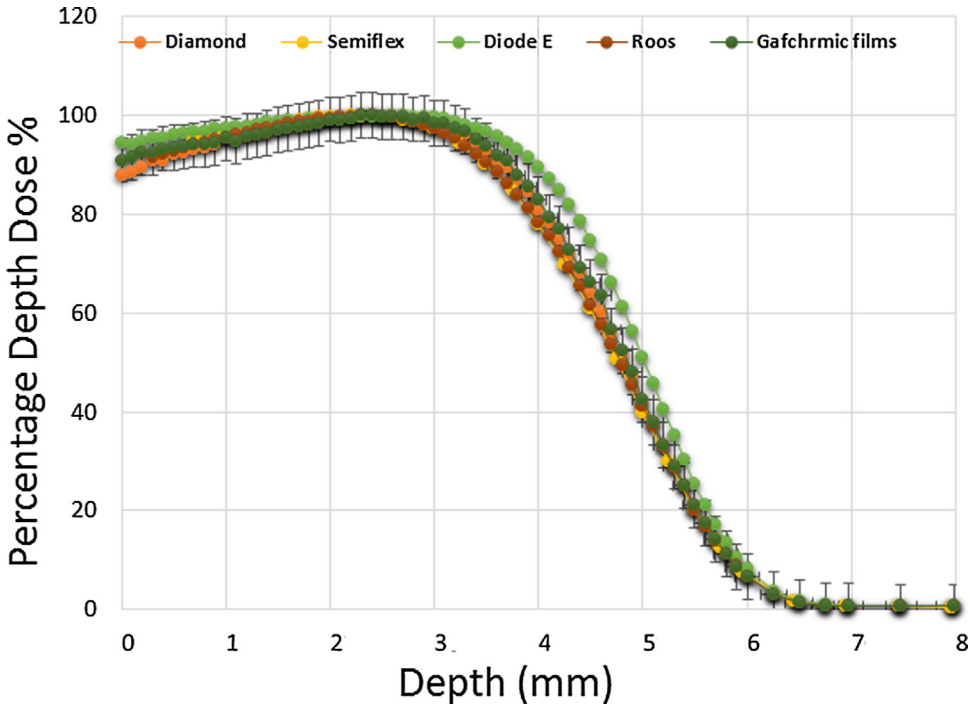

Fig. 3. PDD measurements of the 12 Mev electron beam with the flat applicator (5.5 cm diameter) using gafchromic films with its uncertainties and different detectors (Roos champer, Diamond, Diode-E, 0.125 cm^3 Semiflex chamber).

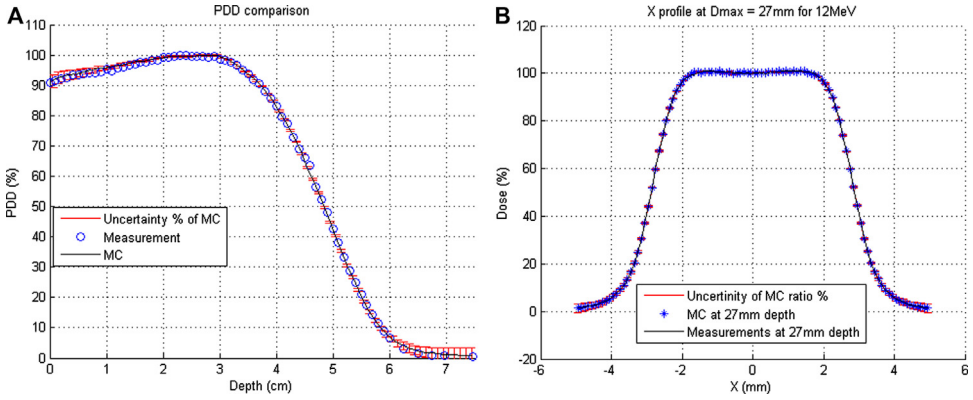

Fig. 4. PDD and dose profile of gafchromic film measurements compared with MC simulations of the 12 MeV with the 5.5 cm diameter of the flat applicator.

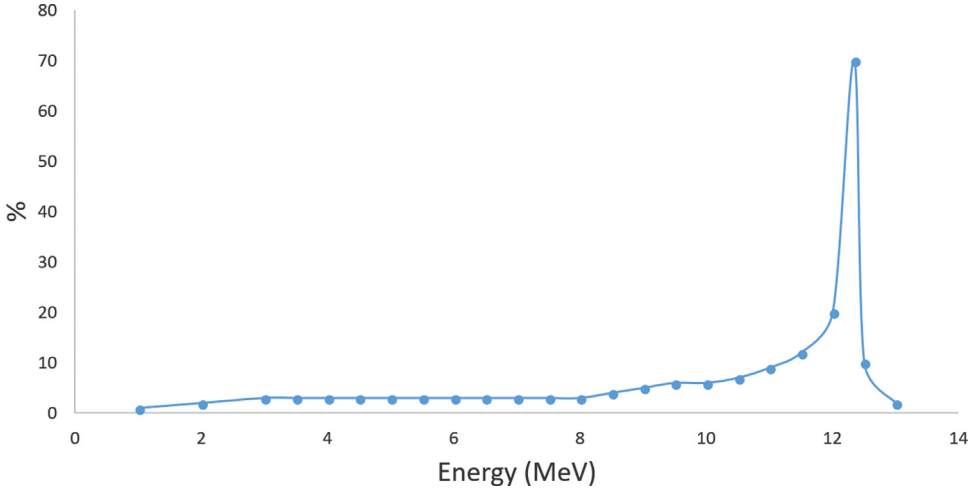

Fig. 5. Spectrum of nominal energy 12 MeV electrons, which emit from electron source in MC model of Mobetron 1000. Move it to supplementary material as asked by the editor.

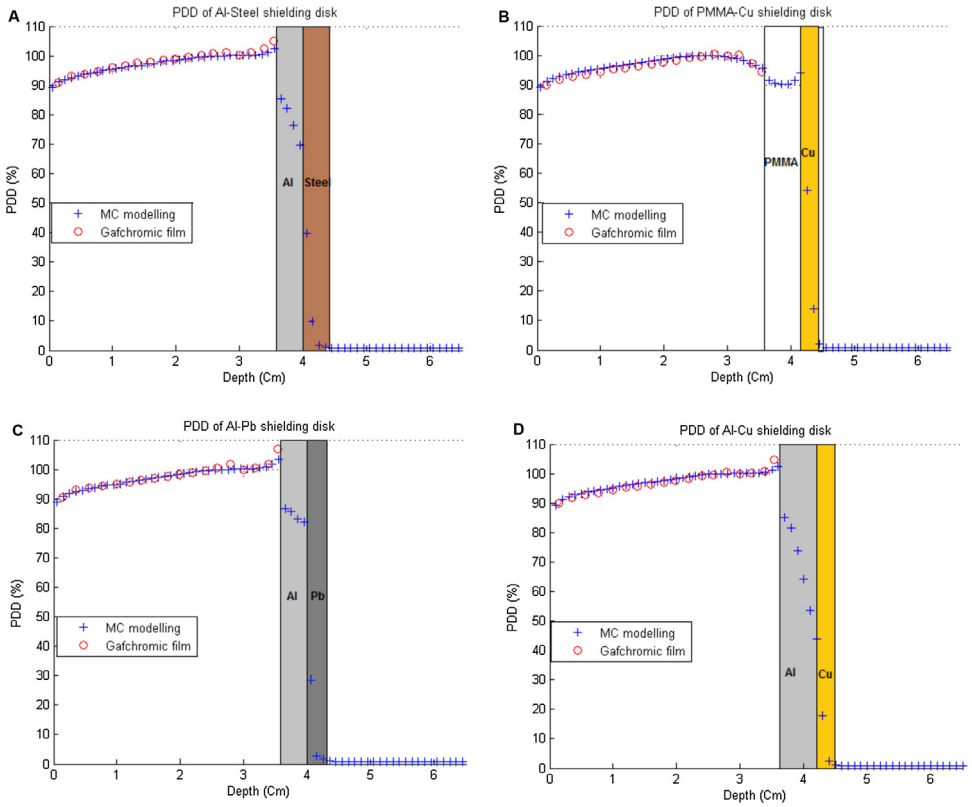

Fig. 6. PDD of MC modeling and gafchromic films measurements with shielding disks. a: Al/Steel; b: PMMA/Cu/PMMA; c: Al/Pb; d: Al/Cu. Remove gridlines as asked by the editor.

is difficult because it requires the opening of the linear accelerator and the removal of most of its internal parts [33]. The first MC model of the Mobetron was done by Janssen et al. [34]. The parameters of the initial electrons source of his model were optimized iteratively until a good match between MC and measurement data was obtained. This is a time consuming approach though.

The method described in the current paper optimizes the weight of mono-energetic measured and calculated PDDs. This requires a limited amount of time and a minimal set of calculations. A 2.2% RMSD obtained in the current work is acceptable taking into account the statistical uncertainty of the MC and the uncertainties on gafchromic film measurements. These are related to many parameters such as: the homogeneity of the sensitive material on the films, the position of the films during the irradiation and the response of the scanner.

The four shielding disks studied have been chosen as they are available in our clinic.

The measurements of gafchromic films for the treatment setup agree with the MC simulation results. The total uncertainty for the red channel is 3.2% but without considering relative orientation of the film nor the homogeneity on the bed of the scanner [35]. The 6 mm PMMA layer absorbs most of the backscatter radiation coming from the copper layer. This is observed for the PDD of the PMMA/Cu/PMMA shielding disk. Oshima et al. analyzed PDD curves in a water phantom for a flat applicator with a 12 MeV beam and they found that the 7 mm PMMA/3 mm Cu disk has no effect on the PDD [36].

Kamomae et al. and Fujimoto et al. have recommended using a flexible paper of Tungsten as shielding disk even if it produces backscatter radiation in the target volume [37,38]. Martignano et al. did a similar study to ours considering other materials and found that a shielding disk of (6 mm Al/3 mm Cu) attenuates the electron beam completely with minimum negligible backscatter radiation [8].

This is not the case for the aluminum layer, since 3 or 4 mm thickness is not enough to absorb the backscatter radiation from lead, steel or copper (Al/Steel, Al/Pb, Al/Cu). All the studied shielding disks stop the incoming beam. The dose values are close to zero beyond the studied disks. Even if the PMMA/Cu/PMMA disk has the minimum surface dose; the surgeon cannot use a shielding disk of 10 mm for some clinical cases. A good compromise between the thickness of the shielding disk and the dose at its surface is the 7 mm Al/Pb disk. A 105% dose is clinically acceptable as the Al/Pb disk is the thinnest of the studied shielding disks. If the surgeon needs a thinner shielding disk, a disk composed of a single material like steel or copper can be considered, accepting a higher surface dose on the. Some centers avoid the use of the lead material inside the patient's body even after sterilization. The diameter of the disk should be larger than the diameter of the applicator but not too much to allow easy insertion inside the patient's body. For example, in our practice, we use a shielding disk that has a diameter that is approximately 1.5 cm larger than the applicator diameter. All our results depend on the maximum energy of the electron beam at the exit window (12.43 MeV). They cannot be generalized to all IOERT linear accelerators as some of them are characterized by higher energies.

The simulation of the electron beam of the Mobetron 1000 accelerator was carried out by using the EGSnrc MC code for the maximum energy of the machine. The tuning process provided good results by using an optimization technique of "least squares superposition".

Dosimetric characterizations of four shielding disks, (8 mm Al/Steel, 7 mm Al/Pb, 10 mm PMMA/Cu/PMMA and 9 mm Al/Cu), were verified using MC simulation and gafchromic films

measurements. It is possible to use any of them clinically, while the best shielding disk is Al/Pb since it has minimum thickness and a small backscatter component.

5. Conclusions

The dose values above and under the shielding disks were acceptable for the four studied shielding types. It is possible to use any of them clinically, while the best shielding disk was the Al/Pb since it has minimum thickness and a small backscatter enhancement. Using only 1 layer of high Z material like lead could stop the beam but the backscatter will increase the dose to tissue above it.

Disclosure of interest

The authors declare that they have no competing interest.

Acknowledgement

This work was fully supported by the Radiotherapy Department at the Institute Jules Bordet, Brussels, Belgium.

References

[1] Podgorsak EB. Review of radiation oncology physics: a handbook for teachers and students. Vienna, Austria: International Atomic Energy Agency; 2003.
[2] Catalano M, Agosteo S, Moretti R, Andreoli S. Monte Carlo simulation code in Optimisation of the IntraOperative Radiation Therapy treatment with mobile dedicated accelerator. J Phys 2007;74:012002.
[3] Opera M, Constantin C, Mihailescu D, Borcia C. A Monte Carlo investigation of the influence of the initial electron beam characteristics on the absorbed dose distributions obtained with a 9 Mev IOERT accelerator. U.P.B. Sci Bull 2012;74:153–66.
[4] Calvo FA, Meirino RM, Orecchia R. Intraoperative radiation therapy first part: rationale and techniques. Crit Rev Oncol Hematol 2006;59:106–15.
[5] Krengli M, Calvo FA, Sedlmayer F, Sole CV, Fastner G, Alessandro M, et al. Clinical and technical characteristics of intraoperative radiotherapy: Analysis of the ISIOERT-Europe database. Strahlenther Onkol 2013;189:729–37.
[6] Severgnini M, de Denaro M, Bortul M, Vidali C, Beorchia A. In vivo dosimetry and shielding disk alignment verification by EBT3 GAFCHROMIC film in breast IOERT treatment. J Appl Clin Med Phys 2014;16:5065.
[7] Beddar AS, Biggs PJ, Chang S, Ezzell GA, Faddegon BA, Hensley FW, et al. Intraoperative radiation therapy using mobile electron linear accelerators: report of AAPM Radiation Therapy Committee Task Group No. 72. Med Phys 2006;33:1476–89.
[8] Martignano A, Menegotti L, Valentini A. Monte Carlo investigation of breast intraoperative radiation therapy with metal attenuator plates. Med Phys 2007;34:4578–84.
[9] Neto AJD, Haddad CMK, Pelosi EL, Zevallos-Chavez JY, Yoriyaz H, Siqueira PDTD. Monte Carlo simulation as an auxiliary tool for electron beam quality specification for intra-operative radiotherapy. Braz J Phys 2005;35:801–4.
[10] Russo G, Casarino C, Arnetta G, Candiano G, Stefano A, Alongi F, et al. Dose distribution changes with shielding disc misalignments and wrong orientations in breast IOERT: a Monte Carlo – GEANT4 and experimental study. J Appl Clin Med Phys 2012;13:1526–9914.
[11] Pentiricci A, Paolucci M, Rossi G, Di Lorenzo R, Felici G, Ciccotelli A. Two shielding protection disks systems in breast intraoperative irradiation. Phys Med 2016;32:321–35.
[12] Hanna S, Barros A, Andrade F, Bevilacqua JLB, Roberto MP, Josa P, et al. Intraoperative Radiation Therapy in Early Breast Cancer Using a Linear Accelerator Outside of the Operative Suite: An "Image-Guided" Approach. Int J Radiat Oncol Biol Phys 2014;89:1015–23.
[13] Alhamada H, Simon S, Philippson C, Vandekerkhove C, Jourani Y, Pauly N, et al. Shielding disk position in intra-operative electron radiotherapy (IOERT): A Monte Carlo study. Phys Med 2018:1–6.
[14] Beddar AS, Krishnan S. Intraoperative radiotherapy using a mobile electron LINAC: a retroperitoneal sarcoma case. J Appl Clin Med Phys 2005;6:95–107.
[15] Natanasabapathi G. Modern practices in radiation therapy. In: Lamanna E, Gallo A, Russo F, Brancaccio R, Soriani A, Strigari L, editors. Intra-Operative Radiotherapy with Electron Beam. INTECH; 2012. p. 145–69.
[16] Loi G, Dominietto M, Cannillo B, Ciocca M, Krengli M, Mones E, et al. Neutron production from a mobile linear accelerator in electron mode for intraopreative radiation therapy. Phys Med Biol 2006;51:695–702.
[17] IntraOp Medical Inc., Santa Clara, CA. Mobile IORT linear accelerator: operator's manual; 1999.
[18] Mills MD, Fajardo LC, Wilson DL, Daves JL, Spanos WJ. Commissioning of a mobile electron accelerator for intraoperative radiotherapy. J Appl Clin Med Phys 2001;2:121–30.
[19] Beddar AS, Domanovic MA, Kubu ML, Ellis RJ, Sibata CH, Kinsella TJ. Mobile linear accelerators for intraoperative radiation therapy. AORN J 2001;74:700–5.
[20] Seco J, Verhaegen F. Monte Carlo Techniques in Radiation Therapy. CRC press; 2013.
[21] Kawrakow I, Mainegra-Hing E, Rogers DWO, Tessier F, Walters BRB. The EGSnrc Code System: Monte Carlo Simulation of Electron and Photon Transport. National Research Council of Canada Report; 2013.
[22] Rogers DWO, Faddegon BA, Ding GX, Ma C-M, We J, Mackie TR. Beam: a Monte Carlo code to simulate radiotherapy treatment units. Med Phys 1995;22:503–24.
[23] Kawrakow I, Walters BRB. Efficient photon beam dose calculations using DOSXYZnrc with BEAMnrc. Med Phys 2006;33:3046–56.
[24] Kawrakow I. Accurate condensed history Monte Carlo simulation of electron transport. EGSnrc, the new EGS4 version. Med Phys 2000;27:485–98.
[25] Bjork P, Knoos T, Nilsson P. Influence of initial electron beam characteristics on Monte Carlo calculated absorbed dose distributions for linear accelerator electron beams. Phys Med Biol 2002;47:4019–41.
[26] Conneely E, Alexander A, Stroian G, Seuntjens J, Foley MJ. An investigation into the use of MMCTP to tune accelerator source parameters and testing its clinical application. J Appl Clin Med Phys 2013;14:3–14.
[27] Iaccarino G, Strigari L, D'Andrea M, Bellesi L, Felici G, Ciccotelli A, et al. MC simulation of electron beams generated by a 12 MeV dedicated mobile IOERT accelerator. Phys Med Biol 2011;56:4579–96.
[28] El Baroukya J, Fournier-Bidoza N, Mazala A, Faresb G, Rosenwalda J-C. Practical use of Gafchromic EBT films in electron beams for in-phantom dose distribution measurements and monitor units verification. Phys Med 2011;27:81–8.
[29] Su FC, Liu Y, Saatsakis S, Shi C, Esquivel C, Papanikolaou N. Dosimetry characteristics of GAFCHROMIC® EBT film responding to therapeutic electron beams. Appl Radiat Isot 2007;65:1187–92.
[30] Chiu-Tsao ST, Ho Y, Shankar R, Wang L, Harrison LB. Energy dependence of response of new high sensitivity radiochromic films for megavoltage and kilovoltage radiation energies. Med Phys 2005;32:3350–4.
[31] Zeidan OA, Stephenson SAL, Meeks SL, Wagner TH, Willoughby TR, Kupelian PA, et al. Characterization and use of EBT radiochromic film for IMRT dose verification. Med Phys 2006;33:4064–72.
[32] Fiandra C, Ricardi U, Ragona R, Anglesio S, Giglioli FR, Calamia E, et al. Clinical use of EBT model Gafchromic film in radiotherapy. Med Phys 2006;33:4314–9.
[33] Stancic V, Secerov B, Ljubenov V. A unified approach to deconvolution radiation spectra measured by radiochromic films. Nuclear technology and radiation protection 2002;17:37–43.
[34] Marroquin EY, Herrera JA, Gonzalez, Camacho Lopez MA, Barajas JE, Garcia-Garduno OA. Evaluation of the uncertainty in an EBT3 film dosimetry system utilizing net optical density. J Appl Clin Med Phys 2016;17:466–81.
[35] Janssen RW, Faddegon BA, Dries WJ. F. Prototyping a large field size IORT applicator for a mobile linear accelerator. Phys Med Biol 2008;53:2089–102.
[36] Oshima T, Aoyama Y, Shimozato T, Sawaki M, Imai T, Ito Y, et al. An experimental attenuation plate to improve the dose distribution in intraoperative electron beam radiotherapy for breast cancer. Phys Med Biol 2009;54:3491–500.
[37] Kamomae T, Monzen H, Kawamura M, Okudaira K, Nakaya T, Mukoyama T, et al. Dosimetric feasibility of using tungsten-based functional paper for flexible chest wall protectors in intraoperative electron radiotherapy for breast cancer. Phys Med Biol 2018;63:015006 [10pp].
[38] Fujimoto T, Monzen H, Nakata M, Okada T, Yano S, Takakura T, et al. 2014 Dosimetric shield evaluation with tungsten sheet in 4, 6, and 9MeV electron beams. Phys Medica 2014;30:838–42.
[39] 9th ISIORT congress abstract book; 2019 http://www.isiort.org/fileadmin/userdaten/dokumente/9th_ISIORT_CONGRESS_ABSTRACT_BOOK.pdf.
[40] Ciocca M, Pedroli G, Orecchia R, Guido A, Cattani F, Cambria R, et al. Radiation survey around a Liac mobile electron linear accelerator for intraoperative radiation therapy. J Appl Clin Med Phys 2009;10:131–8.
[41] Intra M, Luini A, Gatti G, Ciocca M, Gentilini OD, Viana AAC, et al. Surgical technique of intraoperative radiation therapy with electrons (ELIOT) in breast cancer: a lesson learned by over 1000 procedures. Surgery 2006;140:467–71.